Dalton Transactions

ROYAL SOCIETY OF CHEMISTRY

PAPER

View Article Online
View Journal | View Issue

Cite this: *Dalton Trans.*, 2025, **54**, 10890

Reactivity of titanium pyrazolates towards CO_2, CS_2 and N_2O†

Felix Kracht, Sophie Mayer, Cäcilia Maichle-Mössmer and Reiner Anwander *

Received 23rd April 2025,
Accepted 21st June 2025

DOI: 10.1039/d5dt00957j

rsc.li/dalton

The tetravalent titanium pyrazolate $Ti(pz^{Me_2})_4$ inserts two molecules of carbon dioxide instantly at ambient temperature and 1 bar heteroallene, forming the complex $Ti(CO_2{\cdot}pz^{Me_2})_2(pz^{Me_2})_2$ (pz^{Me_2} = 3,5-dimethylpyrazolato). CO_2 insertion is reversible as proven by thermogravimetric analysis (TGA). Solid $Ti(CO_2{\cdot}pz^{Me_2})_2(pz^{Me_2})_2$ exhibits an exceptionally high stability at ambient atmosphere but converts in solution over time *via* deoxygenation into the oxo-bridged species $[Ti(CO_2{\cdot}pz^{Me_2})_2(pz^{Me_2})]_2(\mu\text{-}O)$ and $[Ti(\mu\text{-}O)_2(\mu\text{-}pz^{Me_2})_4(Ti\{CO_2{\cdot}pz^{Me_2}\}\{pz^{Me_2}\})_2]$. Treatment of $Ti(pz^{Me_2})_4$ with CS_2 results in a mono-insertion to $Ti(CS_2{\cdot}pz^{Me_2})(pz^{Me_2})_3$, which is reversible at 110 °C. Applying similar conditions, trivalent $Ti(pz^{tBu_2})_3$ inserts also two molecules of CO_2 to afford $Ti(CO_2{\cdot}pz^{tBu_2})_2(pz^{tBu_2})$ displaying complete de-insertion at 70 °C. At elevated temperatures compound $Ti(CO_2{\cdot}pz^{tBu_2})_2(pz^{tBu_2})$ does neither display redox activity nor engages in a deoxygenation reaction. While tetravalent $Ti(pz^{Me_2})_4$ does not react with N_2O under ambient conditions, trivalent $Ti(pz^{tBu_2})_3$ converts into oxo-bridged $[Ti(pz^{tBu_2})_3]_2(\mu\text{-}O)$ *via* initial N_2O insertion and subsequent fast release of N_2.

Introduction

The rapidly rising greenhouse gas emissions and concomitant record-high concentrations in the Earth's atmosphere are the primary cause for the anthropogenic global climate change, with carbon dioxide (CO_2) having the greatest impact, followed by methane (CH_4) and nitrous oxide (N_2O).[1–13] Although the concentration of N_2O (337.69 ppb, 2024) is relatively low when compared to CO_2 (427 ppm, 2024; 50% increase since start of industrialization), its global warming potential is 300 times stronger, contributing 6% to the anthropogenic greenhouse effect.[1,12,13] The activation of these small, mostly inert molecules leading to their capture, conversion, storage, and ultimately climate change mitigation, has become a major focus of research in the past decades. For the development of efficient capture materials, a fundamental understanding of the activation of such small molecules by metal centres is crucial. In particular, amine-functionalized and M–N(ligand) components/materials feature efficient systems for CO_2 capture and valorization.[14,15]

Titanium is attractive as a sustainable metal, not only because it is affordable and non-toxic, but also because of its high abundance in the Earth's crust. Already in the 1970s, CO_2 insertion into the Ti–N bond of tetravalent $Ti(NMe_2)_4$ under formation of carbamate complex $Ti(CO_2{\cdot}NMe_2)_4$ was reported. However, such carbamate complexes were structurally elucidated only three decades later.[16–18] Similar examples exist for trivalent titanium complexes.[19–21] In addition, a twofold addition of CO_2 across the Ti═N double bond of the tetravalent imide complex $(C_5Me_5)Ti({=}NAr)(L)$ ($Ar = 2,6\text{-}C_6H_3Me_2$; $L = (N\mathit{i}Pr_2)_2CR$; R = Me, Ph) was achieved resulting in $(C_5Me_5)Ti(\{CO_2\}_2{\cdot}NAr)(L)$.[22,23] For sterically less demanding imido ligands, the mono-inserted congener $(C_5Me_5)Ti(CO_2{\cdot}N\mathit{t}Bu)(L)$ ($L = (NR^1)_2CR^2$; $R^1 = SiMe_3$, *i*Pr; R^2 = Ph, Me) was shown to rapidly deoxygenate CO_2 under formation of the oxo-bridged dimer $[(C_5Me_5)Ti(L)(\mu\text{-}O)]_2$ and elimination of the corresponding isocyanate (Scheme 1A).

Light-induced deoxygenation of CO_2 is feasible on a TiO_2 surface in the presence of H_2O under formation of CH_4, CH_3OH, H_2 and O_2,[24,25] whereas CO_2 deoxygenation reactions were also observed for divalent and trivalent titanium compounds.[26,27]

The activation of N_2O with trivalent titanocene complex $(Cp_2TiCl)_2$ has been reported, proceeding *via* slow oxidation of the titanium centre under formation of oxo-bridged species $[Cp_2TiCl]_2O$ and elimination of N_2.[28–31] Only a few examples of N_2O-inserted compounds prior to N_2 elimination have been reported,[28,30] including azoxymetallacylopentene complex $(C_5Me_5)_2Ti(N\{O\}NCPhCPh)$ obtained from $(C_5Me_5)_2Ti(PhCCPh)$ (Scheme 1B).[28]

Institut für Anorganische Chemie, Eberhard Karls Universität Tübingen, Auf der Morgenstelle 18, 72076 Tübingen, Germany.
E-mail: reiner.anwander(at)uni-tuebingen.de

† Electronic supplementary information (ESI) available: Supporting figures, detailed crystallographic data, spectroscopic data (NMR, IR), analytical details. CCDC 2423931–2423936. For ESI and crystallographic data in CIF or other electronic format see DOI: **https://doi.org/10.1039/d5dt00957j**

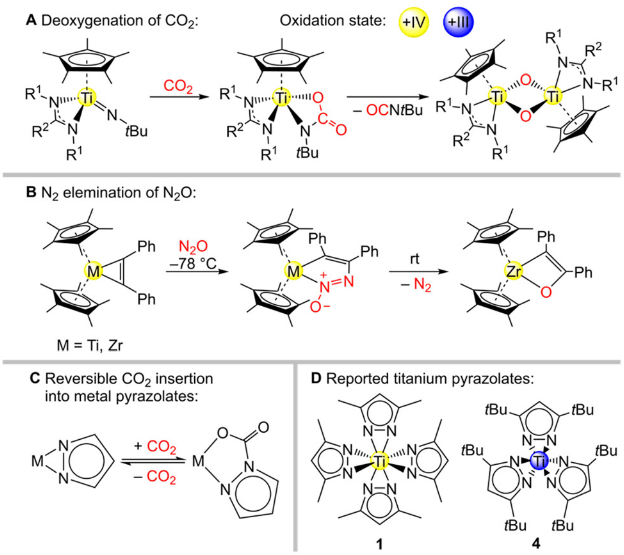

Scheme 1 A: addition of CO_2 across a Ti═N bond and subsequent deoxygenation;[22] B: N_2O insertion into titanium/zirconium complexes and subsequent N_2 elimination;[28] C: reversible CO_2 insertion into metal pyrazolates;[32–34] D: literature-known tetravalent and trivalent homoleptic titanium pyrazolate complexes.[35,36]

Recently, we found that homoleptic metal pyrazolates $[M(pz^{R,R'})_x]$ insert CO_2 readily and reversibly, forming the corresponding carbamate complexes (see Scheme 1C).[32] Structurally characterized examples comprise redox-active $Ce(CO_2{\cdot}pz^{Me_2})_4$, the tetranuclear cluster $[Ce(CO_2{\cdot}pz^{Me_2})_3]_4$, and the light metal derivatives $Mg(CO_2{\cdot}pz^{tBu_2})_2(thf)_2$, $Al(CO_2{\cdot}pz^{tBu_2})_2(pz^{tBu_2})$ and $[Sc(\mu\text{-}CO_2{\cdot}pz^{tBu_2})(pz^{tBu_2})_2]_2$.[33,34] Using unsubstituted $[Mg(pz)_2]_n$, exceptionally high reversible CO_2 capacities of up to 35.7 wt% have been achieved, highlighting its potential as an efficient CO_2 capture material. Spurred by these findings, we envisaged the reactivity of pyrazolate complexes of the light metal titanium toward both carbon dioxide, CS_2 and N_2O. Homoleptic complexes, tetravalent $Ti(pz^{Me_2})_4$ (**1**) and trivalent $Ti(pz^{tBu_2})_3$ (**4**), previously reported by Winter and Mösch-Zanetti, respectively, were chosen as discrete precursors (see Scheme 1D).[35,36]

Results and discussion

CO_2 activation with tetravalent $Ti(pz^{Me_2})_4$

Exposure of tetravalent $Ti(pz^{Me_2})_4$ (**1**) to a 1 bar CO_2 atmosphere in benzene or toluene gave the twofold inserted carbamate complex $Ti(CO_2{\cdot}pz^{Me_2})_2(pz^{Me_2})_2$ ($\mathbf{1}^{\mathbf{CO2}}$) (Scheme 2). The insertion reaction occured instantly, as monitored by an immediate colour change of the solution from yellow to orange. The CO_2 uptake of complex $\mathbf{1}^{\mathbf{CO2}}$ equals a mass fraction of 17.0 wt% CO_2 or 3.8 mmol CO_2 per gram.

A single crystal X-ray diffraction (SCXRD) analysis of $\mathbf{1}^{\mathbf{CO2}}$ revealed two distinct molecules in the unit cell with slightly varying metrical parameters. The four ligands of $\mathbf{1}^{\mathbf{CO2}}$ arrange in a distorted square planar geometry, with the *cis*-positioned carbamato ligands coordinated in the κ^2(N,O) mode (Fig. 1). The pyrazolato ligands are tilted out of the plane spanned by the titanium centre and the two coordinating nitrogen atoms, by 26.6° and 18.9°, respectively. The inserted CO_2 exhibits localized C–O single (1.275(3)–1.277(3) Å) and double bonds (1.205(3)–1.207(3) Å) and OCO angles ranging from 128.5(2) to 129.0(3)°. The loss of aromaticity of the pyrazole ring of the carbamato ligand is indicated by distinct C–C and C–N double/single bonds. Additional CO_2 insertion into $\mathbf{1}^{\mathbf{CO2}}$ is most likely impeded by the coordinative saturation of the small titanium centre, and would cause unfavourable tilting and hence significant steric interference of newly formed carbamato ligands. Fourfold inserted $Ce(CO_2{\cdot}pz^{Me_2})_4$ clearly supports the size-determining influence of the metal centre for CO_2 insertion (effective ionic radii for 6-coordination: Ti^{4+} 0.605, Ce^{4+} 0.87 Å).[37] Although an electronic effect caused by saturation of the titanium centre with two oxygen atoms might play a role as well, this is opposed by the comparatively higher oxophilicity of titanium (θ = 1.0) *versus* cerium (θ = 0.9).[38]

Formation of the twofold inserted complex $\mathbf{1}^{\mathbf{CO2}}$ was confirmed by solution NMR spectroscopy. The ^1H NMR spectrum

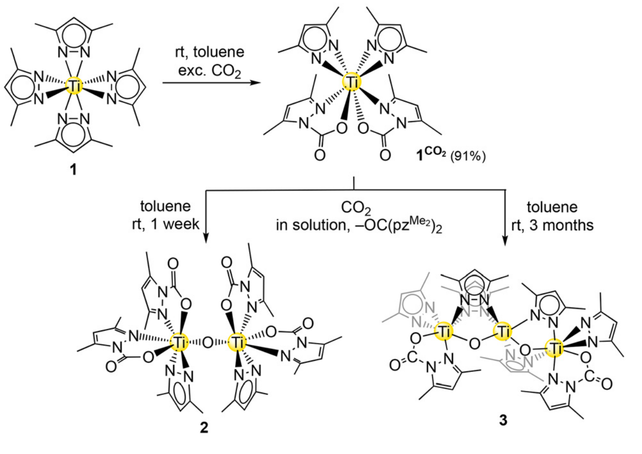

Scheme 2 Reaction of $Ti(pz^{Me_2})_4$ (**1**) with an excess of CO_2 and subsequent deoxygenation in solution affording oxo-bridged species.

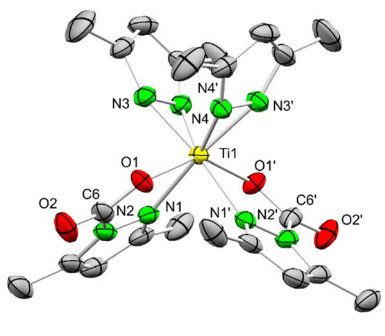

Fig. 1 Crystal structure of $Ti(CO_2{\cdot}pz^{Me_2})_2(pz^{Me_2})_2$ ($\mathbf{1}^{\mathbf{CO2}}$). Ellipsoids are set at the 50% probability level. Hydrogen, lattice toluene and a second molecule of $\mathbf{1}^{\mathbf{CO2}}$ are omitted for clarity. See ESI† for selected interatomic distances and angles.

shows three methyl group signals at δ = 2.62, 2.21 and 2.17 ppm with an integral of 6, 6 and 12 protons, respectively. The two signals at lower field can be assigned to the distinct methyl groups of the two carbamato ligands, caused by CO_2 insertion. The third signal is attributed to the magnetically equal methyl groups of the two unchanged pyrazolato ligands. Further, two signals for the ring protons at δ = 5.72 and 5.00 ppm were detected. The ^{13}C NMR spectrum is consistent with the ^{1}H NMR spectrum and a signal for the inserted CO_2 could be resolved at δ = 150.5 ppm *via* experiments with labelled $^{13}CO_2$ (see Fig. S4†). A diffuse reflectance infrared Fourier transform (DRIFT) measurement revealed a strong band at $\tilde{\nu}$ = 1740 cm^{-1} assigned to the C═O stretching vibration. The CO_2 uptake was corroborated by a thermogravimetric analysis (TGA) showing a CO_2 releasing step of 17.5% between 90–150 °C which is in good agreement with the aforementioned calculated uptake of 17.0 wt%. When solid **1** is exposed to an atmosphere of 1 bar CO_2 a colour change of the powder from yellow to orange was observed. The orange product was identified as $\mathbf{1}^{\mathbf{CO2}}$ by ^{1}H NMR spectroscopy. This can be further interpreted as a fully reversible CO_2 insertion process in the solid state of compound **1**. Application of higher CO_2 pressure of up to 10 bar did not lead to any additional insertion of CO_2 but only the formation of $\mathbf{1}^{\mathbf{CO2}}$. The combination of the small titanium(IV) centre and the steric bulk of the pyrazolato ligand seem to suppress further insertion reactions.

Strikingly, different to our previous studies on magnesium, aluminium and rare-earth-metal pyrazolates, solid $\mathbf{1}^{\mathbf{CO2}}$ remained stable under ambient atmosphere. After one month only small amounts of the hydrolysis product $\text{HOOCpz}^{\text{Me}_2}$ were observed in the ^{1}H NMR spectrum and the solid kept its orange colour (Fig. S6†). In stark contrast, decomposition of $\mathbf{1}^{\mathbf{CO2}}$ readily occurred in solution, both under an argon or CO_2 atmosphere (Fig. S7†). Overnight a new signal set appeared in the ^{1}H NMR spectrum which accumulated over time and after one week only a minor amount of $\mathbf{1}^{\mathbf{CO2}}$ was left. The observed decomposition is reproducible at ambient temperature. The obtained solution provided access to crystals suitable for a SCXRD analysis, which revealed the formation of the oxo-bridged bimetallic complex $[\text{Ti}(\text{CO}_2{\cdot}\text{pz}^{\text{Me}_2})_2(\text{pz}^{\text{Me}_2})]_2(\mu\text{-O})$ (**2**) (Scheme 2 and Fig. S35†). Each titanium centre of **2** is coordinated by two terminal carbamato and one terminal pyrazolato ligand. However, NMR experiments showed the presence of more than one species ruling out a clear signal assignment to **2**. Further, after three months morphologically different crystals formed in the same solution and could be identified by a SCXRD measurement as the oxo-bridged trimetallic complex $[\text{Ti}(\mu\text{-O})_2(\mu\text{-pz}^{\text{Me}_2})_4(\text{Ti}\{\text{CO}_2{\cdot}\text{pz}^{\text{Me}_2}\}\{\text{pz}^{\text{Me}_2}\})_2]$ (**3**, Scheme 2 and Fig. S36†). The central titanium of **3** is bridged by one oxo and two pyrazolato ligands in the μ-N,N mode to each of the outer titanium atoms. The coordination sphere of the outer titanium centres is completed by one terminal pyrazolato ligand in the κ^2(N,N) mode and one carbamato ligand in the κ^2(N,O) mode. The Ti–O(oxo) interatomic distances of **2** and **3** range from 1.790(2) to 1.8199(12) Å with one exception for the inner titanium centre of **3** which is slightly elongated (1.8465(12) Å). The latter is comparable with the reported bis-oxo $[(C_5Me_5)\text{Ti}((\text{NSiMe}_3)_2\text{CPh})(\mu\text{-O})]_2$ (1.8429(13)–1.8604(12) Å) and mono-oxo $[(C_5H_4Me)_2\text{TiCl}]_2\text{O}$ (1.837(2) Å).[23,39] Similarly, the Ti–O(carbamato) interatomic distances of oxo-bridged **2** and **3** are slightly shorter (1.9930(18)–2.0286(19) Å) than in oxo-free $\mathbf{1}^{\mathbf{CO2}}$ (2.0445(18)–2.0484(16) Å), with again one exception detected for **3** (2.0437(13) Å).

Decomposition of $\mathbf{1}^{\mathbf{CO2}}$ was not observed when the solution is kept at 0 °C. Deoxygenation of inserted CO_2 or hydrolysis and a subsequent dissociation of pyrazole/carbamic acid are likely decomposition pathways of $\mathbf{1}^{\mathbf{CO2}}$ (Fig. S42†), which would result in oxo complexes like **2** and **3**. Note that single-crystalline $\mathbf{1}^{\mathbf{CO2}}$ was obtained after three years at −40 °C, while the corresponding ^{1}H NMR spectrum revealed that it remained stable during this time span. This makes a hydrolysis pathway highly unlikely. However, reactions of titanium compounds with CO_2 involving a deoxygenation process and subsequent formation of oxo bridges have been reported previously.[22] Unfortunately, conclusive organic co-products of a putative deoxygenation reaction involving $\mathbf{1}^{\mathbf{CO2}}$ could not be identified by ^{13}C NMR spectroscopy, even when labelled $^{13}CO_2$ was used. The formation of CO was not observed. Mass spectrometry experiments revealed a $[M + H]^+$-fragment of 219.16 g mol^{-1} which fits well to the urea derivative $\text{OC}(\text{pz}^{\text{Me}_2})_2$ (219.12 g mol^{-1}). This is in good agreement with the displacement of two pz^{Me_2}-moieties upon the formation of **2**. Experiments in amber glass NMR tubes showed the same decomposition pattern, excluding a light-induced mechanism. The elongation of the titanium-oxo chain indicates that this decomposition pathway might ultimately lead to the formation of titania, TiO_2. However, it has remained unclear whether trimetallic **3** is formed *via* bimetallic **2**.

CS_2 activation with tetravalent $\text{Ti}(\text{pz}^{\text{Me}_2})_4$

To examine the feasibility of a sulfido-bridged compound similar to complexes **2** or **3**,[40] **1** was reacted with an excess of CS_2. ^{1}H NMR monitoring at ambient temperature indicated a rather slow conversion which was not complete even after several weeks. Therefore, the reaction was conducted at 60 °C affording full conversion to the mono-inserted complex $\text{Ti}(\text{CS}_2{\cdot}\text{pz}^{\text{Me}_2})(\text{pz}^{\text{Me}_2})_3$ ($\mathbf{1}^{\mathbf{CS2}}$) after five days (Scheme 3). The thiocarbamato ligand coordinates to the metal centre in the κ^2(N,S) mode similar to the carbamato ligand in complex $\mathbf{1}^{\mathbf{CO2}}$ (Fig. 2). The C–S interatomic distances of the inserted CS_2 moiety reveal

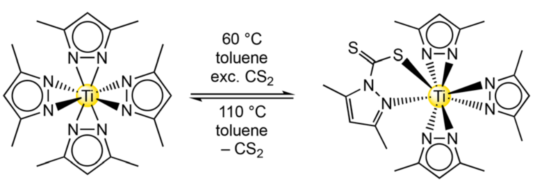

1 $\mathbf{1}^{\mathbf{CS2}}$ (81%)

Scheme 3 Reaction of $\text{Ti}(\text{pz}^{\text{Me}_2})_4$ (**1**) with an excess of CS_2.

localized double and single bonds of 1.6543(19) Å and 1.7019 (19) Å, respectively, forming an angle of 121.64(12)°.

Accordingly, the degree of electron delocalization is comparatively larger in $\mathbf{1}^{\mathbf{CS2}}$ ($\Delta_{\mathrm{C–S}}$ 0.0476 Å) than in $\mathbf{1}^{\mathbf{CO2}}$ ($\Delta_{\mathrm{C–O}}$ 0.068–0.072 Å). An additional insertion of CS_2 seems disfavoured for steric reasons considering the larger size of the sulphur atoms. Moreover, the HSAB mismatch according to Pearson, the low thiophilicity of titanium (S = 0.0),[38] and changed electrophilicity of the heteroallene will counteract a second insertion.

At ambient temperature, the ^{1}H NMR spectrum of $\mathbf{1}^{\mathbf{CS2}}$ shows the thiocarbamato ligand as sharp signals, with the aromatic backbone proton resonating at δ = 5.05 ppm and distinct methyl groups at δ = 2.38 and 2.36 ppm. In the aromatic region two broad signals appeared at δ = 5.75 and 5.61 ppm in a 2 : 1 integral ratio, while the remaining methyl groups gave one broad signal. The integral ratios of the aromatic protons indicate that the pyrazolato ligands positioned *trans* and *cis* to the thiocarbamato ligand are magnetically unequal. Correspondingly, a variable temperature (VT) ^{1}H NMR experiment at −60 °C revealed a sharpening of the broadened resonances resulting in three distinct signals sets with an integral ratio of 1 : 1 : 2, assigned to the thiocarbamato ligand, the *trans*- and the two *cis*-positioned pyrazolato ligands (Fig. S12†). The ^{13}C signal of the inserted CS_2 is resolved at δ = 209.2 ppm being consistent with the literature.[41] In the DRIFT spectrum of $\mathbf{1}^{\mathbf{CS2}}$ vibrations characteristic of C–S double and single bonds are detected in the fingerprint region at $\tilde{\nu}$ = 1071 and 895 cm^{-1}, respectively.[42,43] A TGA experiment revealed a CS_2 releasing step of 14.8% between 110–180 °C, which is close to the theoretical value of 15.1%.

Any decomposition of $\mathbf{1}^{\mathbf{CS2}}$ could not be observed at ambient temperature, while heating to 110 °C led to de-insertion of CS_2 under full recovery of **1**. Again, this is most likely caused by the soft Lewis base character of sulphur, which also disfavours the formation of sulphido bridges. Crucially, complex **1** features a hard titanium(IV) centre featuring a significantly higher oxophilicity (θ = 1.0) than thiophilicity (S = 0.0).[38]

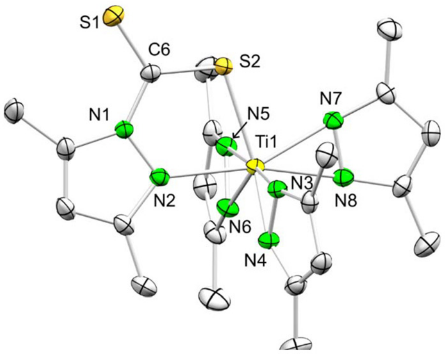

Fig. 2 Crystal structure of Ti(CS_2·pz^{Me_2})(pz^{Me_2})$_3$ ($\mathbf{1}^{\mathbf{CS2}}$). Ellipsoids are set at the 50% probability level. Hydrogen atoms and one toluene lattice are omitted for clarity. See ESI† for selected interatomic distances and angles.

CO_2 and N_2O activation with trivalent Ti(η^2-pz^{tBu_2})$_3$

Exposure of trivalent Ti(pz^{tBu_2})$_3$ (**4**) to a 1 bar CO_2 atmosphere in toluene gave an immediate colour change of the solution from blue over green and yellow to finally red. An SCXRD analysis revealed the formation of the twofold-inserted titanium (III) complex Ti(CO_2·pz^{tBu_2})$_2$(pz^{tBu_2}) ($\mathbf{4}^{\mathbf{CO2}}$) (Scheme 4). The CO_2 uptake of complex $\mathbf{4}^{\mathbf{CO2}}$ amounts to a mass fraction of 13.1 wt% CO_2 or 3.0 mmol CO_2 per gram.

Complex $\mathbf{4}^{\mathbf{CO2}}$ is isostructural to the aluminium complex Al(CO_2·pz^{tBu_2})$_2$(pz^{tBu_2}) reported recently (Fig. 3).[34] Accordingly, two carbamato ligands in the κ^2(N,O) mode and one pyrazolato in the κ^2(N,N) mode adopt a propeller-like geometry with both stereoisomers (Λ,Δ) present in the unit cell. Another CO_2 insertion into the third pyrazolato ligand is impeded by the bulky *t*Bu moieties, which prevent the pyrazolato ligand from the necessary tilting (*cf.*, effective ionic radii for 6-coordination: Ti^{3+} 0.670, Al^{3+} 0.535 Å).[37] The unit cell holds three distinct molecules of $\mathbf{4}^{\mathbf{CO2}}$ and six lattice toluene, which form a superstructure with alternating layers of complex $\mathbf{4}^{\mathbf{CO2}}$ and toluene (Fig. S39†).

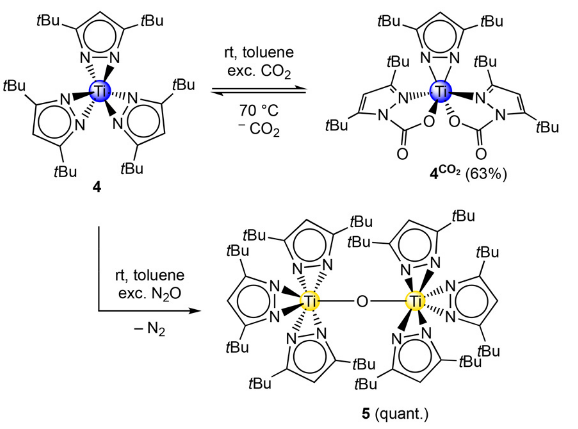

Scheme 4 Reactions of Ti(pz^{tBu_2})$_3$ (**4**) with an excess of CO_2 and N_2O.

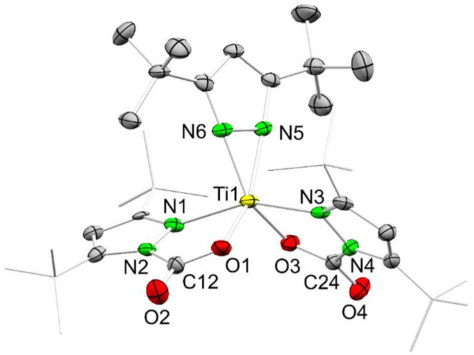

Fig. 3 Connectivity of Ti(CO_2·pz^{tBu_2})$_2$(pz^{tBu_2}) ($\mathbf{4}^{\mathbf{CO2}}$). Ellipsoids are set at the 50% probability level and *t*Bu moieties are displayed in wireframe projection for clarity. Hydrogen atoms, two additional molecules of $\mathbf{4}^{\mathbf{CO2}}$ and six lattice toluene are omitted for clarity.

The DRIFT spectrum of $\mathbf{4^{CO2}}$ shows two characteristic bands for C═O stretching vibration at $\tilde{\nu}$ = 1765 and 1753 cm^{-1} similar to the aluminium congener. Due to the paramagnetic character of $\mathbf{4^{CO2}}$ the signals in the ^1H NMR spectrum are significantly broadened and only two signals are resolved. One very broad signal between δ = 7–3 ppm can most likely be assigned to aromatic protons in the pyrazolato/carbamato backbones while the other broadened signal at δ = 1.55 ppm can be ascribed to *t*Bu moieties. Despite the broadened signals, the CO_2 insertion reaction can be easily monitored by ^1H NMR spectroscopy (Fig. S16†). At the start of the reaction signals for **4** and $\mathbf{4^{CO2}}$ in addition to another signal at δ = 1.67 ppm could be observed. The additional signal likely arises from a mono-inserted product, which was also found for the aluminium congener. The EPR spectrum of $\mathbf{4^{CO2}}$ is shown in Fig. S41.†

After one hour the conversion of **4** to $\mathbf{4^{CO2}}$ is complete, which is also indicated by the red colour of the solution. A VT ^1H NMR study revealed a complete CO_2 release already at 70 °C suggesting that the overall CO_2 insertion process into **4** is reversible (Fig. S18†). This is again also indicated by the colour of the solution which turns blue after the experiment and again red after several hours at ambient temperature. Shining UV light on compound $\mathbf{4^{CO2}}$ led to oxidation of the titanium centre, however, the formation of a significant amount of oxalate was not observed by ^{13}C NMR spectroscopy. A TGA experiment revealed an initial toluene solvent release of 13.9% between 77–110 °C, which is in line with the high lattice toluene content in the crystalline material. Subsequently, a CO_2 releasing step of 12.1% between 110–150 °C was observed. Both releasing steps fit to a toluene/$\mathbf{4^{CO2}}$ ratio of 1 : 1 (toluene: 12.0%; CO_2: 11.5%). Interestingly, different to tetravalent $\mathbf{1^{CO2}}$ no deoxygenation reaction was observed for $\mathbf{4^{CO2}}$ over time in solution, however, a fast decomposition of neat $\mathbf{4^{CO2}}$ occurred at ambient atmosphere to unidentified products.

Treatment of tetravalent **1** with an excess of N_2O led to no visible reaction as suggested by ^1H NMR spectroscopy and the unchanged yellow colour of the solution. In contrast, exposure of trivalent **4** to N_2O resulted in an immediate colour change from blue to green and after 10 minutes to yellow. A ^1H NMR spectrum revealed the presence of a paramagnetic (not **4**) and a diamagnetic species. Overnight, orange crystals formed in a toluene solution and a SCXRD measurement revealed the formation of the oxo-bridged species $[Ti(pz^{tBu_2})_3]_2(\mu\text{-}O)$ (**5**) (Scheme 4). Both titanium centres of **5** underwent N_2O-promoted +III → +IV oxidation under elimination of N_2. The ^1H NMR spectrum of the supernatant solution revealed a full conversion of **4** to **5**, while the signals of the new paramagnetic species disappeared completely. The latter paramagnetic species is most likely the elusive N_2O insertion complex in which the titanium centre is still in the formal oxidation state +III. So far, attempts to isolate this paramagnetic species were not successful.

The connectivity structure of **5** indicates a highly symmetrical structure with only one symmetrically independent pyrazolato ligand, the titanium centre and bridging oxygen in the asymmetric unit (Fig. 4).

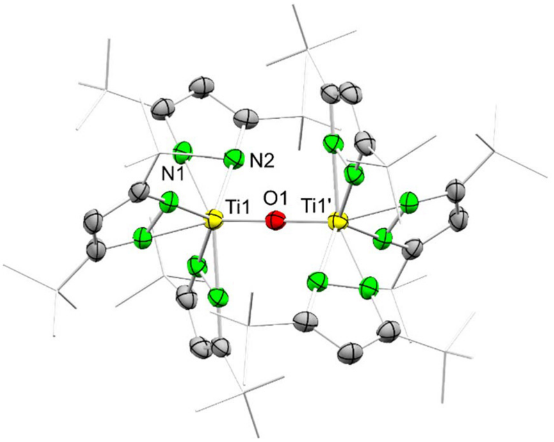

Fig. 4 Connectivity of $[Ti(pz^{tBu_2})_3]_2(\mu\text{-}O)$ (**5**). Ellipsoids are set at the 50% probability level. Hydrogen atoms are omitted and *t*Bu moieties are displayed in the wireframe projection for clarity.

Each titanium centre is coordinated by three terminal pyrazolato ligands in the κ^2(N,N) mode adopting a propeller-like geometry. NMR studies corroborate the highly symmetric character of **5** showing only one signal set for all six pyrazolato ligands. The ^1H NMR spectrum displays a sharp signal at δ = 6.36 ppm with an integral of six protons assignable to the aromatic ring protons and a slightly broadened signal at δ = 1.01 ppm with an integral of 108 protons for the *t*Bu moieties. Similarly, the ^{13}C NMR spectrum revealed one signal set, however, the quaternary carbon ring atom could only be resolved in a ^1H–^{13}C HMBC NMR experiment at δ = 157.5 ppm.

The core structure of **5** is reminiscent of **2** except the inserted CO_2. Therefore, we wondered about whether **5** can be transformed into putative $\{[Ti(CO_2{\cdot}pz^{tBu_2})_2(pz^{tBu_2})]_2(\mu\text{-}O)\}$ or $\{[Ti(CO_2{\cdot}pz^{tBu_2})(pz^{tBu_2})_2]_2(\mu\text{-}O)\}$ when exposed to an excess of CO_2. Due to the insolubility of **5** in non-donating solvents these experiments were conducted in THF, which however did not result in any CO_2 insertion at ambient conditions as indicated by ^1H NMR experiments. This behaviour can be ascribed to the enhanced steric bulk of the *t*Bu moieties blocking the titanium centres, in addition to the low solubility of **5** in THF. Attempts to synthesize the sterically less demanding $Ti(pz^{Me_2})_3$ as a precursor in order to access putative $[Ti(pz^{Me_2})_3]_2(\mu\text{-}O)$ were not successful.

Catalytic formation of cyclic carbonates

Titanium complexes are widely used in the copolymerization of CO_2 and epoxides.[44–48] Since metal pyrazolates effectively promote the catalytic cycloaddition of CO_2 and epoxides, a similar behaviour of the titanium derivatives could be anticipated.[32–34] For better comparability, the conditions of the catalytic transformations were adapted to our previous studies (Scheme 5).

Tetravalent $Ti(pz^{Me_2})_4$ (**1**) exhibits moderate catalytic activity for the conversion of propylene oxide (59%), ranging between

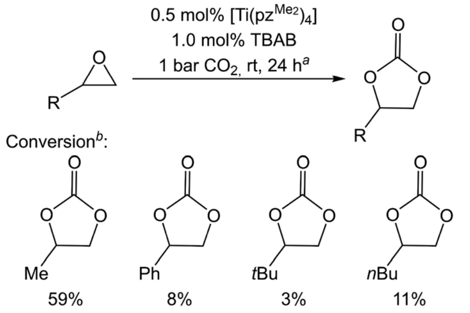

Scheme 5 Catalytic conversion of CO_2 and epoxide into cyclic carbonates by applying titanium pyrazolate **1** as catalyst. [a]Reaction conditions: 1 bar CO_2, 0.5 mol% catalyst (**1** and **2**), 1 mol% tetra-*n*-butylammonium bromide (TBAB) as cocatalyst at ambient temperature for 24 h in neat epoxide; [b]Conversion determined by comparison of the integral protons at the α-position of the epoxide and the corresponding cyclic carbonate (exception: 2-*tert*-butyloxirane/3,3-dimethyl-1,2-butene carbonate where the integral of the *t*Bu moieties was used).

magnesium (42–59%) and rare-earth-metal pyrazolates (84–99%) and close to $Al(pz^{tBu_2})_3$ (65%).[32–34] This is in line with the carboxopilicity criterion (as derived from the CO_2-release temperature),[33] and reflects both the enhanced oxophilicity and Lewis acidity of titanium(IV).[41] As expected, the conversion of sterically more demanding epoxides was considerably lower, being lowest for 2-*tert*-butyloxirane (3%) and highest for epoxy hexane (11%). Trivalent $Ti(pz^{tBu_2})_3$ (**4**) showed a significantly lower conversion of 27% for propylene oxide compared to tetravalent **1**. This can be ascribed to side reactions, as indicated by an immediate colour change upon the addition of epoxide. Trivalent titanium compounds are known to catalytically convert epoxides to alcohols under ring opening and oxidation of the titanium center.[49] Examples of titanium-based catalysts in this cycloaddition reaction are rather rare.[50–55] The highest catalytic activity was observed for the tetrazole containing $(C_5Me_5)TiCl_2(O,N\text{-L})$ (L = 5-(2-hydroxyphenolate)-1*H*-tetrazole) featuring a maximum TOF of 422 for propylene oxide at 75 °C and 22 bar CO_2.[52] Recently, the Ti_{31} cluster $(C_2H_8N)_8[Ti_{31}O_{52}(OiPr)_4(PhCO_2)_{24}]$ was reported to reach a quantitative conversion for propylene oxide when a catalyst load of 0.83 mol% is used at 80 °C and 1 bar CO_2 over five days, according to a photocatalytic mechanism.[55]

Conclusions

Tetravalent $Ti(pz^{Me_2})_4$ undergoes a twofold CO_2 insertion to $Ti(CO_2{\cdot}pz^{Me_2})_2(pz^{Me_2})_2$ when exposed to an excess of CO_2 as proven by SCXRD, NMR and DRIFT experiments. A thermogravimetric analysis showed an exhaustive CO_2 release between 90–150 °C pointing to the reversibility of the CO_2 insertion. In solid form, $Ti(CO_2{\cdot}pz^{Me_2})_2(pz^{Me_2})_2$ showed an exceptionally high stability, when compared to derivatives of other light metals. Even after a month at ambient atmosphere only minor hydrolysis products were observed. Strikingly, in solution under a 1 bar CO_2 atmosphere $Ti(CO_2{\cdot}pz^{Me_2})_2(pz^{Me_2})_2$ converted into oxo-bridged species $[Ti(CO_2{\cdot}pz^{Me_2})_2(pz^{Me_2})]_2(\mu\text{-O})$ and $[Ti(\mu\text{-O})_2(\mu\text{-}pz^{Me_2})_4(Ti\{CO_2{\cdot}pz^{Me_2}\}\{pz^{Me_2}\})_2]$, *en route* to titania. This transformation reflects the highly polarizing nature of titanium(IV) and is accelerated at elevated temperatures. Heteroallene CS_2 undergoes a fully reversible mono-insertion into $Ti(pz^{Me_2})_4$ *via* formation of $Ti(CS_2{\cdot}pz^{Me_2})(pz^{Me_2})_3$. The thiocarbamate complex does not engage in the formation of sulfido-bridged species, even under thermal treatment. Trivalent $Ti(pz^{tBu_2})_3$ also undergoes a twofold CO_2 insertion and the obtained bis(carbamato) complex $Ti(CO_2{\cdot}pz^{tBu_2})_2(pz^{tBu_2})$ is stable in solution against oxidation and deoxygenation. $Ti(CO_2{\cdot}pz^{tBu_2})_2(pz^{tBu_2})$ de-inserts CO_2 exhaustively already at 70 °C without a decomposition side reaction. Distinct reactivity of tetravalent $Ti(pz^{Me_2})_4$ and trivalent $Ti(pz^{tBu_2})_3$ is also found when treated with nitrous oxide. The tetravalent pyrazolate displayed inert behaviour toward N_2O, whereas $Ti(pz^{tBu_2})_3$ gets oxidized to afford the oxo-bridged complex $[Ti(pz^{tBu_2})_3]_2(\mu\text{-O})$ *via* fast release of N_2.

Conflicts of interest

There are no conflicts of interest.

Data availability

The data that support the findings of this study are available in the ESI† of this article.

Acknowledgements

We are grateful to the VECTOR foundation for generous support. We thank Adrian Jenner for performing the EPR measurement, Dr Markus Ströbele for running the TGA experiments and Dr Peter Haiss for running the mass spectrometry experiments.

References

1 H. Lee and J. Romero, *IPCC, 2023: Climate Change 2023: Synthesis Report. Contribution of Working Groups I, II and III to the Sixth Assessment Report of the Intergovernmental Panel on Climate Change*, Geneva, Switzerland, 2023, pp. 35–115.

2 P. Falkowski, R. J. Scholes, E. Boyle, J. Canadell, D. Canfield, J. Elser, N. Gruber, K. Hibbard, P. Högberg, S. Linder, F. T. Mackenzie, B. Moore III, T. Pedersen, Y. Rosenthal, S. Seitzinger, V. Smetacek and W. Steffen, The Global Carbon Cycle: A Test of Our Knowledge of the Earth as a System, *Science*, 2000, **290**, 291–296.

3 S. Solomon, G.-K. Plattner, R. Knutti and P. Friedlingstein, Irreversible climate change due to carbon dioxide emissions, *Proc. Natl. Acad. Sci. U. S. A.*, 2009, **106**, 1704–1709.

4 R. S. Haszeldine, Carbon Capture and Storage: How Green Can Black Be?, *Science*, 2009, **325**, 1647–1652.

5 D. W. Keith, Why Capture CO_2 from the Atmosphere, *Science*, 2009, **325**, 1654–1655.

6 G. Centi and S. Perathoner, Opportunities and prospects in the chemical recycling of carbon dioxide to fuels, *Catal. Today*, 2009, **148**, 191–205.

7 M. Cokoja, C. Bruckmeier, B. Rieger, W. A. Herrmann and F. E. Kühn, Transformation of Carbon Dioxide with Homogeneous Transition-Metal Catalysts: A Molecular Solution to a Global Challenge, *Angew. Chem., Int. Ed.*, 2011, **50**, 8510–8537.

8 N. von der Assen, P. Voll, M. Peters and A. Bardow, Life cycle assessment of CO_2 capture and utilization: a tutorial review, *Chem. Soc. Rev.*, 2014, **43**, 7982–7994.

9 M. Aresta, A. Dibenedetto and A. Angelini, Catalysis for the Valorization of Exhaust Carbon: from CO_2 to Chemicals, Materials, and Fuels. Technological Use of CO_2, *Chem. Rev.*, 2014, **114**, 1709–1742.

10 Q. Liu, L. Wu, R. Jackstell and M. Beller, Using carbon dioxide as a building block in organic synthesis, *Nat. Commun.*, 2015, **6**, 5933.

11 R. E. Siegel, S. Pattanayak and L. A. Berben, Reactive Capture of CO_2: Opportunities and Challenges, *ACS Catal.*, 2023, **13**, 766–784.

12 M. J. Prather, Time Scales in Atmospheric Chemistry: Coupled Perturbations to N_2O, NO_y, and O_3, *Science*, 1998, **279**, 1339–1341.

13 T. S. Ledley, E. T. Sundquist, S. E. Schwartz, D. K. Hall, J. D. Fellows and T. L. Killeen, Climate Change and Greenhouse Gases, *EOS., Trans. AGU*, 1999, **80**, 453–458.

14 A. C. Forse and P. J. Milner, New chemistry for enhanced carbon capture: beyond ammonium carbamates, *Chem. Sci.*, 2021, **12**, 508–516.

15 R. Ayyappan, I. Abdalghani, R. C. D. Costa and G. R. Owen, Recent developments on the transformation of CO_2 utilising ligand cooperation and related strategies, *Dalton Trans.*, 2022, **51**, 11582–11611.

16 C. Forte, M. Hayatifar, G. Pampaloni, A. M. R. Galletti, F. Renili and S. Zacchini, Ethylene Polymerization Using Novel Titanium Catalytic Precursors Bearing *N*,*N*-Dialkylcarbamato Ligands, *J. Polym. Sci., Part A: Polym. Chem.*, 2011, **49**, 3338–3345.

17 M. H. Chisholm and M. W. Extine, Reactions of Transition Metal-Nitrogen σ Bonds. 3. Early Transition Metal *N*,*N*-Dimethylcarbamates. Preparation, Properties, and Carbon Dioxide Exchange Reactions, *J. Am. Chem. Soc.*, 1977, **99**, 782–792.

18 M. H. Chisholm and M. W. Extine, Reactions of Transition Metal-Nitrogen σ Bonds. 4. Mechanistic Studies of the Carbon Dioxide Insertion and Carbon Dioxide Exchange Reactions Involving Early Transition Metal Dimethylamido and *N*,*N*-Dimethylcarbamato Compounds, *J. Am. Chem. Soc.*, 1977, **99**, 792–802.

19 A. Mendiratta, C. C. Cummins, F. A. Cotton, S. A. Ibragimov, C. A. Murillo and D. Villagrán, A Diamagnetic Ditatanium(III) Paddlewheel Complex with No Direct Metal–Metal Bond, *Inorg. Chem.*, 2006, **45**, 4328–4330.

20 D. B. Dell'Amico, F. Calderazzo, U. Girulani and G. Pelizzi, *N*,*N*-Dialkylcarbamato complexes of titanium(III) and vanadium(III), *Gazz. Chim. Ital.*, 1986, **116**, 609–611.

21 D. B. Dell'Amico, F. Calderazzo, U. Giurlani and G. Pelizzi, Synthesis and Reactivity of *N*,*N*-Dialkylcarbamato Complexes of Titanium(III) and Vanadium(III). Crystal and Molecular Structure of an Anionic Dimeric Titanium(III) Derivative, *Chem. Ber.*, 1987, **120**, 955–964.

22 A. E. Guiducci, C. L. Boyd, E. Clot and P. Mountford, Reactions of cyclopentadienyl-amidinate titanium imido compounds with CO_2: cycloaddition-extrusion *vs.* cycloaddition-insertion, *Dalton Trans.*, 2009, 5960–5979.

23 P. J. Tiong, A. Nova, L. R. Groom, A. D. Schwarz, J. D. Selby, A. D. Schofield, E. Clot and P. Mountford, Reactions of Cyclopentadienyl-Amidinate Titanium Hydrazides with CO2, CS2, and Isocyanates: Ti=N_α Cycloaddition-NNR$_2$ Group Transfer Reactions, *Organometallics*, 2011, **30**, 1182–1201.

24 M. Anpo and K. Chiba, Photocatalytic reduction of CO_2 on anchored titanium oxide catalysts, *J. Mol. Catal.*, 1992, **74**, 207–212.

25 M. Anpo, H. Yamashita, Y. Ichihashi and S. Ehara, Photocatalytic reduction of CO_2 with H_2O on various titanium oxide catalysts, *J. Electroanal. Chem.*, 1995, **396**, 21–26.

26 A. F. R. Kilpatrick and F. G. N. Cloke, Reductive deoxygenation of CO_2 by a bimetallic titanium bis(pentalene) complex, *Chem. Commun.*, 2014, **50**, 2769–2771.

27 G. Fachinetti, C. Floriani, A. Chiesi-Villa and C. Guastini, Carbon Dioxide Activation. Deoxygenation and Disproportionation of Carbon Dioxide Promoted by Bis(cyclopentadienyl)titanium and -zirconium Derivatives. A Novel Bonding Mode of the Carbonato and a Trimer of the Zirconyl Unit, *J. Am. Chem. Soc.*, 1979, **101**, 1767–1775.

28 G. A. Vaughan, C. D. Sofield, G. L. Hillhouse and A. L. Rheingold, Oxygen-Atom Transfer from Nitrous Oxide. Identification of Intermediates in the Oxidation of Diphenylacetylene at Group 4 Metal Centers and the Structural Characterization of $(\eta\text{-}C_5Me_5)_2Ti\{N(O)NCPh{=}CPH\}\cdot 1/2\ C_7H_8$, *J. Am. Chem. Soc.*, 1989, **111**, 5491–5493.

29 D. J. Mindiola, L. A. Watson, K. Meyer and G. L. Hillhouse, Functionalization of Complexed N_2O in Bis(pentamethylcyclopentadienyl) Systems of Zirconium and Titanium, *Organometallics*, 2014, **33**, 2760–2769.

30 Y. Liang, I. Efremenko, Y. Diskin-Posner, L. Avram and D. Milstein, Calcium-Ligand Cooperation Promoted Activation of N_2O, Amine, and H_2 as well as Catalytic Hydrogenation of Imines, Quinoline, and Alkenes, *Angew. Chem., Int. Ed.*, 2024, **63**, e202401702.

31 F. Bottomley, I. J. B. Lin and M. Mukaida, Reactions of Dinitrogen Oxide (Nitrous Oxide) with Dicyclopentadienyltitanium Complexes Including a Reaction in Which Carbon Monoxide Is Oxidized, *J. Am. Chem. Soc.*, 1980, **102**, 5238–5242.

32 U. Bayer, D. Werner, C. Maichle-Mössmer and R. Anwander, Effective and Reversible Carbon Dioxide

Insertion into Cerium Pyrazolates, *Angew. Chem., Int. Ed.*, 2020, **59**, 5830–5836.

33 F. Kracht, P. Rolser, K. Eichele, C. Maichle-Mössmer and R. Anwander, Carbon dioxide affinity ("carboxophilicity") of trivalent light metal pyrazolates, *Inorg. Chem. Front.*, 2024, **11**, 6948–6959.

34 F. Kracht, P. Rolser, P. Preisenberger, C. Maichle-Mössmer and R. Anwander, Organomagnesia: Reversibly High Carbon Dioxide Uptake by Magnesium Pyrazolates, *Adv. Sci.*, 2024, **11**, 2403295.

35 N. C. Mösch-Zanetti, R. Krätzner, C. Lehmann, T. R. Schneider and I. Usón, Titanium(III) Compounds with η^2-Pyrazolato Ligands, *Eur. J. Inorg. Chem.*, 2000, 13–16.

36 I. A. Guzei, A. G. Baboul, G. P. A. Yap, A. L. Rheingold, H. B. Schlegel and C. H. Winter, Surprising Titanium Comnplexes Bearing η^2-Pyrazolato Ligands: Synthesis, Structure, and Molecular Orbital Studies, *J. Am. Chem. Soc.*, 1997, **119**, 3387–3388.

37 R. D. Shannon, Revised Effective Ionic Radii and Systematic Studies of Interatomic Distances in Halides and Chalcogenides, *Acta Cryst. A*, 1976, **32**, 751–767.

38 K. P. Kepp, A Quantitative Scale of Oxophilicity and Thiophilicity, *Inorg. Chem.*, 2016, **55**, 9461–9470.

39 Y. Le Page, J. D. McCowan, B. K. Hunter and R. D. Heyding, The crystal and molecular structure of bis(biscyclopentadienylchlorotitanium)oxide, *J. Organomet. Chem.*, 1980, **193**, 201–207.

40 A. F. R. Kilpatrick, J. C. Green and F. G. N. Cloke, The Reductive Activation of CO_2 Across a Ti=Ti Double Bond: Synthetic, Structural, and Mechanistic Studies, *Organometallics*, 2015, **34**, 4816–4829.

41 H. L. M. Van Gaal, J. W. Diesveld, F. W. Pijpers and J. G. M. Van der Linden, ^{13}C NMR Spectra of Dithiocarbamates. Chemical Shifts, Carbon–Nitrogen Stretching Vibration Frequencies, and π Bonding in the NCS_2 Fragment, *Inorg. Chem.*, 1979, **18**, 3251–3260.

42 D. M. Wiles, B. A. Gingras and T. Suprunchuk, The C=S stretching vibration in the infrared spectra of some thiosemicarbazones, *Can. J. Chem.*, 1967, **45**, 469–473.

43 S. Jaiswal, S. K. Pandey, J. Prajapati, S. Chandra, M. K. Gond, M. K. Bharty, I. Tiwari and R. J. Butcher, Cd(II) complexes derived from thiazoline, hydrazide and carbodithioate ligands: synthesis, crystal structures and electrochemical sensing of uric acid, *Appl. Organomet. Chem.*, 2023, **37**, e7085.

44 K. Nakano, K. Kobayashi and K. Nozaki, Tetravalent Metal Complexes as a New Family of Catalysts for Copolymerization of Epoxides with Carbon Dioxide, *J. Am. Chem. Soc.*, 2011, **133**, 10720–10723.

45 C. C. Quadri and E. Le Roux, Copolymerization of cyclohexene oxide with CO_2 catalyzed by tridentate N-heterocyclic carbene titanium(IV) complexes, *Dalton Trans.*, 2014, **43**, 4242–4246.

46 S. K. Raman, A. C. Deacy, L. Pena Carrodeguas, N. V. Reis, R. W. F. Kerr, A. Phanopoulos, S. Morton, M. G. Davidson and C. K. Williams, Ti(IV)–Tris(phenolate) Catalyst Systems for the Ring-Opening Copolymerization of Cyclohexene Oxide and Carbon Dioxide, *Organometallics*, 2020, **39**, 1619–1627.

47 I. Sancho, M. Navarro, M. Montilla, P. Salvador, C. Santamaría, J. M. Luis and A. Hernán-Gómez, Ti(III) Catalysts for CO_2/Epoxide Copolymerization at Unusual Ambient Pressure Conditions, *Inorg. Chem.*, 2023, **62**, 14873–14887.

48 L. Suresh, R. Lalrempuia, T. Fjermestad, K. W. Törnroos, J. Bour, G. Frache, A. Nova and E. Le Roux, Trapping of Key "Ate" Intermediates of NHC-Group IV Relevant to Catalyzing Copolymerization of Cyclohexene Oxide with CO_2, *Organometallics*, 2025, **44**, 68–81.

49 C. Yao, T. Dahmen, A. Gansäuer and J. Norton, Anti-Markovnikov alcohols via epoxide hydrogenation through cooperative catalysis, *Science*, 2019, **364**, 764–767.

50 D. Bai, H. Jing, Q. Liu, Q. Zhu and X. Zhao, Titanocene dichloride-Lewis base: An efficient catalytic system for coupling of epoxides and carbon dioxide, *Catal. Commun.*, 2009, **11**, 155–157.

51 D. Bai, G. Nian, G. Wang and Z. Wang, Titanocene dichloride/KI: an efficient catalytic system for synthesis of cyclic carbonates from epoxides and CO_2, *Appl. Organomet. Chem.*, 2013, **27**, 184–187.

52 M. J. Go, K. M. Lee, C. H. Oh, Y. Y. Kang, S. H. Kim, H. R. Park, Y. Kim and J. Lee, New Titanium Catalysts Containing Tetrazole for Cycloaddition of CO_2 to Epoxides, *Organometallics*, 2013, **32**, 4452–4455.

53 Y. Wang, Y. Qin, X. Wang and F. Wang, Coupling reaction between CO_2 and cyclohexene oxide: selective control from cyclic carbonate to polycarbonate by ligand design of salen/salalen titanium complexes, *Catal. Sci. Technol.*, 2014, **4**, 3964–3972.

54 F. Al-Qaisi, E. Streng, A. Tsarev, M. Nieger and T. Repo, Titanium Alkoxide Complexes as Catalysts for the Synthesis of Cyclic Carbonates from Carbon Dioxide and Epoxides, *Eur. J. Inorg. Chem.*, 2015, 5363–5367.

55 C. Liu, Y. Liu, G. Zhang, D. Wang, G. Chen, F. Gao, L. Liu, C.-H. Tung and Y. Wang, Seed-Mediated Growth of a High-nuclearity Titanium-oxide Cluster with Enhanced Photocatalytic Activities in CO_2/Epoxide Cycloaddition, *Eur. J. Inorg. Chem.*, 2024, **27**, e202400189.